Surface acoustic wave actuated cell sorting (SAWACS)

T. Franke, Susanne Braunmüller, L. Schmid, Achim Wixforth, D. A. Weitz

Surface acoustic wave actuated cell sorting (SAWACS)†

T. Franke,*[ab] S. Braunmüller,[b] L. Schmid,[b] A. Wixforth[b] and D. A. Weitz[a]

We describe a novel microfluidic cell sorter which operates in continuous flow at high sorting rates. The device is based on a surface acoustic wave cell-sorting scheme and combines many advantages of fluorescence activated cell sorting (FACS) and fluorescence activated droplet sorting (FADS) in microfluidic channels. It is fully integrated on a PDMS device, and allows fast electronic control of cell diversion. We direct cells by acoustic streaming excited by a surface acoustic wave which deflects the fluid independently of the contrast in material properties of deflected objects and the continuous phase; thus the device underlying principle works without additional enhancement of the sorting by prior labelling of the cells with responsive markers such as magnetic or polarizable beads. Single cells are sorted directly from bulk media at rates as fast as several kHz without prior encapsulation into liquid droplet compartments as in traditional FACS. We have successfully directed HaCaT cells (human keratinocytes), fibroblasts from mice and MV3 melanoma cells. The low shear forces of this sorting method ensure that cells survive after sorting.

Introduction

Cell sorting is of tremendous importance not only for basic cell biology but also for clinical medicine, cancer research, reproductive medicine or transplantation immunology.[1,2] Modern cell sorting schemes operate in two different ways: Cells are either sorted in continuous flow or encapsulated in small liquid droplets prior to sorting.[3,4] In the latter case the problem of sorting applies to the droplets and not to the cells. Drops can be sorted in air or in another immiscible continuous liquid. Traditional fluorescence activated cell sorters encapsulate cells in drops in air which are then labelled with an electric charge and subsequently separated in an electric field. These sorters reach very high sorting rates but have several disadvantages including high costs and large dead volume which make it impossible to separate cells from small sample volumes. Moreover, elaborate cleaning and maintenance procedures are necessary to prevent cross-contamination of different samples, making handling more difficult. These drawbacks can be avoided using low cost disposable microfluidic devices which operate at small sample volumes. In such devices, highly monodisperse aqueous droplets enclosing the cells can be produced at very high rates in an immiscible continuous oil phase instead of air. Such emulsions[5] can even be prepared of higher hierarchy in so called multiple emulsions containing drops in drops.[6-8] In single emulsions, the objects to be sorted can be easily distinguished from the bulk solution because of their inherent contrast in material properties of the aqueous and oil phases. This contrast can be exploited for the sorting mechanism. Most commonly used is the polarizability

contrast in dielectrophoretic sorters.[9] This technique has recently proven to be able to sort at rates as high as 2 kHz.[10] However, all droplet enhanced sorters come with an additional processing step of loading cells into the drops.[11] In some cases, enclosing the cells in drops may not be desirable; for example, if the cells are to be cultured after sorting, they must be first removed from the emulsion.

In contrast to droplet sorting, direct cell-sorting schemes operating in the continuous phase have to deal with low contrast of material properties of cells and bulk as both are typically aqueous liquids. To overcome this limitation, responsive beads are often biochemically attached to the cells to enhance the separation efficiency. In magnetic activated cell sorting (MACS) a magnetic bead is selectively adhered to a target cell prior to sorting in a magnetic field. Also, attachment of polarizable beads has been used to subsequently separate the target and waste cells in an electric field gradient. Optical force switching[12] has been used for sorting as well but suffers from relatively slow sorting rates. There are a few techniques that utilize hydrodynamic flow to sort cells such as syringe enhanced pumping or electrokinetic mobilization.[13,14] Typically, they all suffer from slow response times and consequently low sorting rates or low cell viability under high electric fields.

Our technique combines the advantage of fast cell sorting of FACS in the kHz regime with the advantages of microfluidic technology. It operates in continuous flow without enclosing cells in drops or labelling them with responsive beads prior to separation. We use a low cost disposable microfluidic polydimethylsiloxane (PDMS) device with a tiny dead volume and we can handle total process volumes as small as ~100 μl. The sorting is fully electronically controlled and integrated on the microfluidic chip. Because we actuate a hydrodynamic flow in bulk, the shear stress on the cells is minimized and cells remain viable after sorting.

The physical principle of the technique we exploit is based on an effect called "acoustic streaming".[15,16] We use surface acoustic

---

[a]Department of Physics and School of Engineering and Applied Science, Harvard University, Cambridge, USA
[b]University of Augsburg Experimentalphysik I, Microfluidics Group, Augsburg, Germany
† Electronic supplementary information (ESI) available: Micrograph of murine fibroblasts taken at the outlet of the SAW sorting device. See DOI: 10.1039/b915522h

waves (SAW) to drive microflows in the PDMS channels. As long as the SAW propagates on the surface of the substrate it is barely damped. However, when the substrate is covered with water the wave irradiates energy into the liquid which gives rise to internal streaming of the fluid. The effect has been utilized to actuate drops on open surfaces[17] and in closed channels[18] and to enhance mixing.[19,20] This streaming effect differs significantly from another commonly used technique which employs standing surface acoustic waves[21] (SSAW) which can be used to align and wash particles.[22-24] However, the underlying physical principle is completely different: In SSAW, a stationary standing wave is built up and objects are driven to positions of larger or smaller wave amplitude according to their compressibility contrast with respect to the suspending medium.[25] This force is often termed as acoustic radiation force and is induced by an ultrasonic standing wave field.[26-28] Acoustic radiation force acting on an interface between two liquids with different densities can also be used to actuate the heterogeneous fluid itself.[28] By contrast, in our device we actuate the homogeneous continuous fluid including the objects and no contrast in compressibility, dielectric constant or density is required.[18]

Experimental setup

SAW – PDMS hybrid device

The hybrid sorting device we present in this article directs cells by acoustic streaming induced by a surface acoustic wave on a piezoelectric substrate. We excite the surface acoustic wave by an interdigitated transducer (IDT). The IDT consists of two gold electrodes deposited onto the piezoelectric substrate, each with a comb-like interdigitated-finger structure. The operating frequency of the IDT is determined by the ratio of the sound velocity in the substrate to twice the finger spacing. The IDT has a tapered shape with a decreasing finger repeat distance varying from 23 to 28 μm. This provides a particularly narrow wave path width for the sound wave propagating on the substrate because the finger spacing only obeys the resonance condition at one position. The frequency was varied between 140 MHz and 150 MHz, which corresponds to a finger spacing of 25.4 μm to 27.3 μm. The gold electrodes are produced by vapour deposition and standard lithography. The anisotropic piezoelectric substrate is a Y-cut $LiNbO_3$ with the crystal axis rotated around the X-axis by 128° (128° Y-Cut). The fingers of the IDT are carefully aligned perpendicular to the X-axis and the alternating RF frequency therefore excites a Rayleigh wave propagating in the direction of the X-axis. To apply the high frequency voltage we use a GHz-signal generator (Wavetek, Model 3010) and subsequently amplify the signal to a power of ∼30 dBm. To assemble the microfluidic hybrid device, both the PDMS mould and the piezo-substrate were treated in ozone plasma and carefully assembled on top of each other under a microscope. The enclosed PDMS channel with a height of 50 μm and three inlets is fabricated using soft lithography. The fluid in the main channel, which contains the cells, is hydro-dynamically focussed by the fluid from the two side inlets to align the cells horizontally, and cells are subsequently sorted in one of the two outlet channels. The IDT is positioned directly beside the channel and cells flow into the collect or waste channel depending on the actuation state
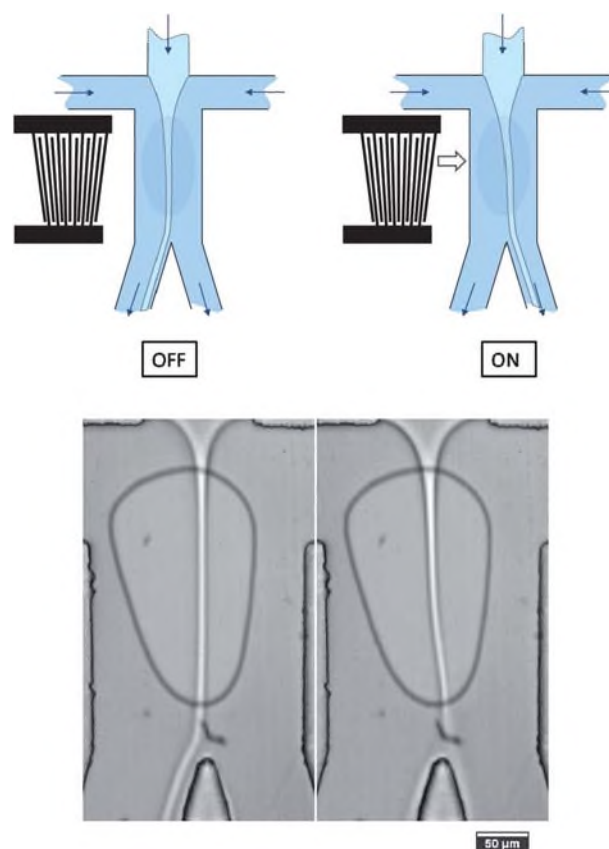
Fig. 1 Schematic illustrations and corresponding phase contrast micrographs of the surface-acoustic-wave-actuated PDMS hybrid chip for cell sorting (top views): The main channel is hydrodynamically focused by adjusting the flows through two side channels. Without applying a surface acoustic wave the jet of the main channel moves into the left outlet channel due to its lower hydrodynamic resistance. Schematic illustration and phase contrast micrograph (OFF, left). When switching on the SAW, acoustic streaming is induced and deflects the focussing stream into the right channel outlet (ON, right). Because cells are only in the focused region of the flow they can be directed into the designated channel. The dark blue and the light grey region in the schematic illustration and the micrograph respectively are the areas of contact of PDMS mould and piezo-substrate.

of the IDT as shown in Fig. 1. The bonded PDMS–SAW hybrid device is mounted on the stage of an inverted fluorescence microscope and imaged by a fast camera (Photron, Fastcam 1024 PCI).

Cell sample preparation

We demonstrate the usefulness of the device for cell sorting with three different cell types: HaCaT cells (humane keratinocytes, Biochrom AG, Berlin), murine fibroblasts L929 cells (obtained from S. Thalhammer, Munich) and MV3 melanoma cells (obtained from S. Schneider, Münster). The HaCaT cells and the murine fibroblasts were maintained in RPMI medium (Biochrom AG), the MV3-cells in MEM medium (PAA). All media were supplemented with 10% fetal bovine serum (PAA) and 1% streptavidin/penicillin. Confluent cells were harvested with Trypsin/EDTA. For sorting experiments, cells were

resuspended in a 0.85% (w/v) NaCl solution, buffered with Hepes (30 mM) containing 1% (w/v) BSA and 14% OptiPrep (Sigma-Aldrich) density gradient medium to increase buoyancy for density matching. The sheath buffer was PBS (pH 7.4) only.

Operating principle

The SAW deflects the flow only in a small region between y_{ON} and y_{OFF} as highlighted in blue in Fig. 2. The action of the surface acoustic wave input on the acoustic streaming is instantaneous on a ms-time scale, but because the blue region of SAW coupling and the sorting junction at the origin of the x–y coordinate system in Fig. 2 do not coincide its effect on sorting is delayed by the time that it takes for the deflected fluid flow to reach the sorting junction.

To illustrate the sorting principle and correlate the input signal (power on/off) of the SAW to the output signal, which is the deflection of the focussed jet, we consider a square wave input as shown in Fig. 2. The period T of the square wave is given by the square wave modulation frequency f_{IDT} of the interdigital transducer $T = 1/f_{IDT}$ and determines the sorting rate. In the experiment we have varied this frequency f_{IDT} between 100 Hz and 2 kHz.

Such a signal causes a x-deflection at position $y = 0$ as shown in the right schematic plot: the onset of SAW pulse is at time $t = 0$, and has no immediate x-deflection, $x = x_{min}$ (jet flows in left outlet channel). Instead, the action of the SAW causes deflection at this position only after a delay of $t_{delay} = y_{off}/v_{flow}$, with flow velocity v_{flow}, because the diversion in the flow has to travel downstream. This is followed by a linear increase in deflection up to the maximum at $t = y_{on}/v_{flow}$. At that time a particle with initial position $y = y_{on}$ at $t = 0$ passes the branch at $y = 0$. This maximal deflection $x = x_{max}$ lasts until the SAW power is switched off again at $t = T/2$, whereupon the flow follows the reverse characteristics of the deflection profile. The maximum and minimum deflections can be controlled by the flow of side channels and the SAW power, while the flow velocity v_{flow} can be adjusted by the inlet flow rates.
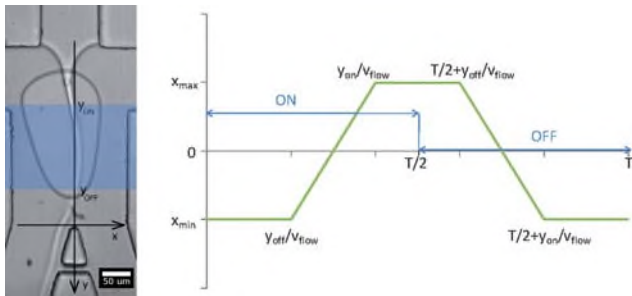

Fig. 2 Micrograph of a deflected hydrodynamically focussed jet (left image) and schematic of the time dependence of jet deflection in the microchannel caused by switching a square wave "ON" and "OFF" (right image). The blue square wave is the input signal (square wave modulation of SAW) and the green line corresponds to the output signal (fluid jet deflection). The origin of the x–y coordinate is set to be at the branch of the waste and collect channels. The y-direction is the flow direction of the liquid flow and the x-direction is the direction of deflection due to an applied SAW. Shaded in blue is the region where the SAW is acting on the jet (left image).

Results

Periodically alternating the amplitude of the surface acoustic wave causes the focussed jet to deflect with the same frequency as the modulation frequency of the exciting SAW. A cell moving from the main channel is aligned within this jet and follows the flow downstream as shown in Fig. 3. We carefully adjust the position of the jet prior to the sorting experiment by controlling the pressure of the sheath flows with the SAW off. This procedure is critical to the sorting ratio of cells in the left and right channel for periodically oscillating excitation. For instance, if one intends a 1 : 1 sorting in both outlets, necessarily $x_{min} = -x_{max}$ (see also Fig. 2).
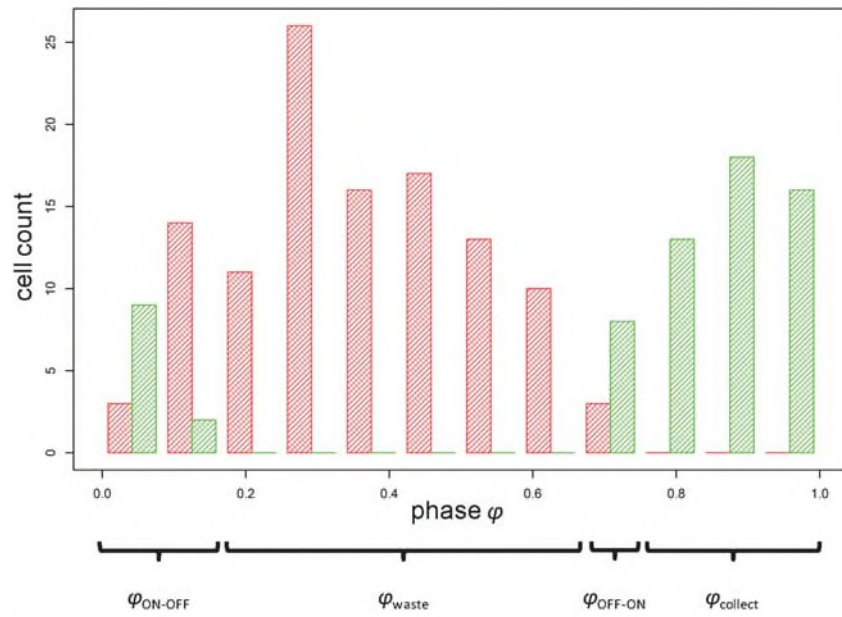
We evaluate the sorting efficiency by the number of cells sorted into the collect and waste channel respectively. We apply a periodically oscillating square wave signal depending on time to the IDT and vary its frequency f_{IDT} from 100 Hz to 2 kHz. Here, one would expect cells to be periodically sorted into the collect channel when the SAW is switched on and into the waste channel when the SAW is switched off. We characterize the time dependence by the phase angle. The phase angle is the time since the last switch off of the SAW divided by the period T. For each frequency we count the number of cells falling into one of the channels as a function of the corresponding phase angle φ. We find experimentally that for one phase angle interval all cells are directed in the collect channel while for another interval all cells enter the waste channel without exception (100% sorting efficiency). We denote the length of these intervals by $\varphi_{collect}$ and φ_{waste}, respectively. In between $\varphi_{collect}$ and φ_{waste} are intervals where cells enter both the collect and waste channel at the same phase angle. We define these transient intervals where sorting is ambiguous by φ_{ON-OFF} and φ_{OFF-ON}. We have found that the length of these transient intervals increases with sorting frequency while the lengths of $\varphi_{collect}$ and φ_{waste} decrease. At a critical sorting frequency the transient intervals expand over the complete phase angle range (sorting efficiency <100%). A typical experiment at 1 kHz oscillation frequency is shown in Fig. 4 together with a complete list summarising all the experiments with different cell types and frequencies. Hence, an integrated cell sorter with an automated detector should be operated below the critical frequency. The width of the transient intervals also yields an estimation of the critical sorting frequency: The width of the transient interval in Fig. 4 is ~3/12f thus we estimate a critical frequency of 4 kHz. At this frequency the transient interval is expected to expand over all phase angles. We have achieved a sorting rate of 2 kHz experimentally with 100% efficiency.

We demonstrate the inherent gentleness of our method with a cell viability test. From a stock solution of the fluorophore Calcein AM in dimethyl sulfoxide (DMSO, 5 mg/ml) we added 2 μl to 1 ml cell suspension. Calcein AM is retained in cells that have intact membranes and gives rise to a fluorescent signal; however, it does not label dead cells, and is rapidly lost under conditions that cause cell lysis.[29,30] This property allows us to evaluate the viability of cells which have passed through the SAW sorting device (see ESI†). Among the cells which have passed the sorting device we detect 93% viable cells as compared to 97% viability of reference sample of murine fibroblasts which have not passed through the device. For the HaCat
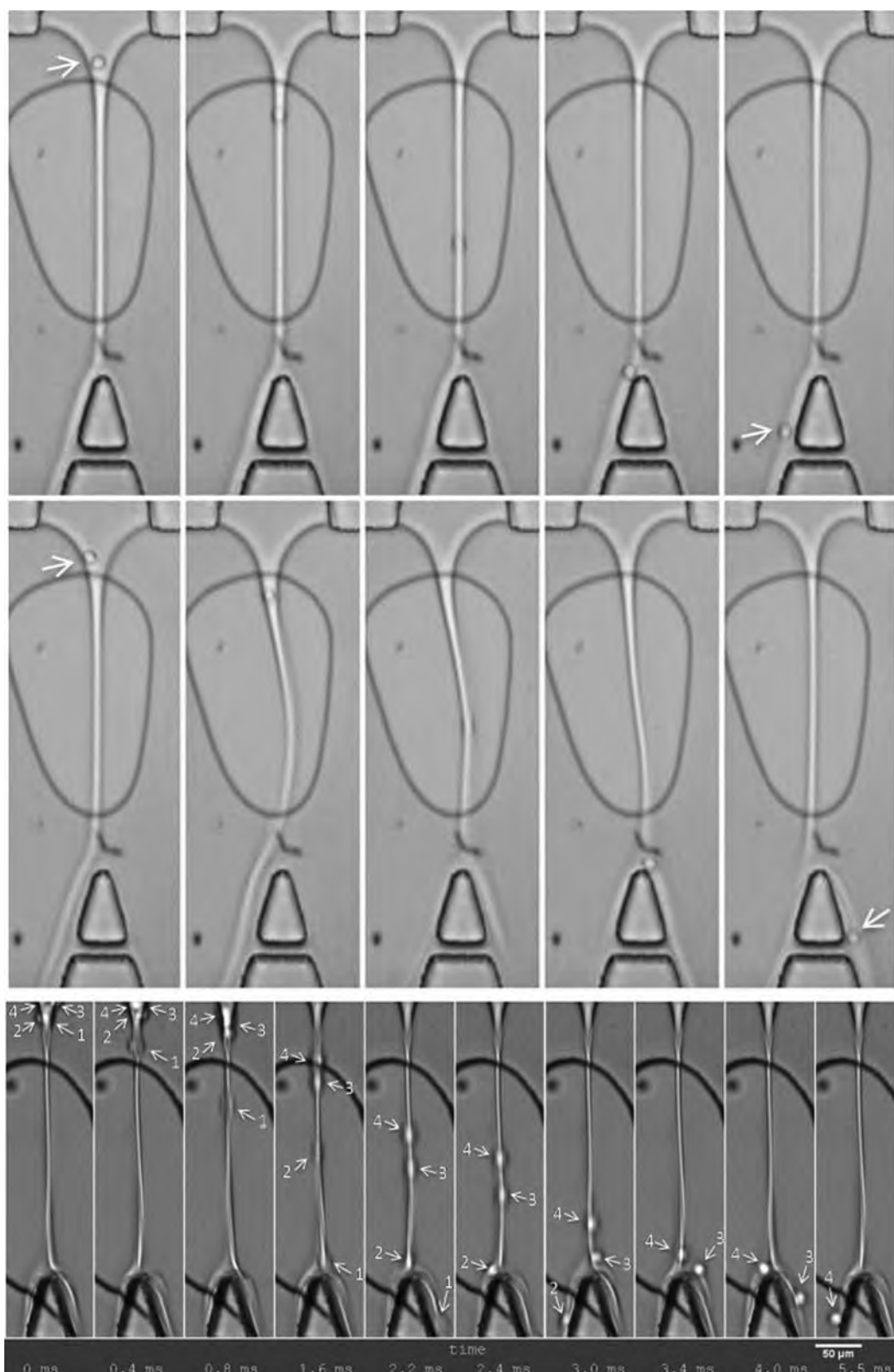
Fig. 3 Cell sorting in two outlets upon application of a periodically oscillating SAW amplitude. (Upper row) A cell entering the sorting region moves through the left channel if the SAW is switched off (default channel). (Middle row) After application of an electrical voltage to the IDT the excited SAW bends the jet and diverts the cells into the right collect channel. The micrographs are taken at time intervals of 2 ms. (Lower row) Micrograph of MV3 cells sorted at 1 kHz. Cells entering the flow focussed area of the device from the top, in very close proximity, with three cells in contact. However, they get separated as the flow field of the hydrodynamic cell focussed region is accelerated, and successively move through different outlet channels. The distance attained between the cells is sufficient to alternately sort them at high frequency into the right and left outlet.

Fig. 4 (Upper histogram) Sorting efficiency of the acoustic sorter operating at 2 kHz sorting frequency (2 times oscillation frequency) is shown in a cell count histogram. Counts were summarized over a small interval ($1/12f_{IDT}$) and displayed by bars. Cells deflected in the collect channel (green) and the default channel (red, waste) when the SAW is applied are shown. Note that for phases within the intervals denoted as $\varphi_{collect}$ and φ_{waste} all collected cells enter the respective channel without exception (100% efficiency). Only at the small transient regions close to $\varphi = 0$ and $\varphi = 0.65$ do we find cells within both channels. The width of the intervals $\varphi_{collect}$ and φ_{waste} differ because the cell-transporting jet is not optimally adjusted for $x_{min} = -x_{max}$ (see also discussion Fig. 3). (Lower table) Sorting efficiency dependence on sorting rate for different cell types. For lower frequencies sorting efficiency was 100% and all cells within the respective phase interval $\varphi_{collect}$ and φ_{waste} were collected in the waste or collect channel. At high frequencies sorting was imperfect (lower than 100%) and no intervals $\varphi_{collect}$ and φ_{waste} for perfect sorting could be defined. Here, we divide the phase range into only two intervals $\varphi_{collect}$ and φ_{waste} and neglect the transient intervals φ_{ON-OFF} and φ_{OFF-ON} (values are in brackets in the table). We define the collect and waste efficiency by the ratio of correctly sorted cells to the total number of cells falling into the corresponding interval. The highest 100%-efficient sorting rate was found for fibroblasts to be 2 kHz.

cells 94% of the cells passing the sorter were viable as compared to a control reference of 97% viability. This confirms the low shear forces on the cells due to the flow induced by the SAW device.

Conclusion

In summary, we demonstrate a novel sorting scheme operating at high sorting rates of several kHz and demonstrate sorting of diverse types of cells including HaCaT cells, fibroblasts from mouse and MV3 melanoma cells. The gentleness of our method is proven with a cell viability test. Due to the low dead volume, as little as 100 µl cell suspension is sufficient. Our SAW hybrid device is particularly useful when only small sample volumes are available and when a high viability of sorted cells is desired. Furthermore, because the sorting operates in continuous flow, subsequent culturing of cells can be easily accomplished. The sorting scheme is fully assembled on a microfluidic chip and can be simply integrated into a more complex chip design, such as with repeated sorting steps or other functional modules. Its low cost and disposability makes it an ideal tool for analysis in research as well as diagnostics.

References

1 M. Eisenstein, *Nature*, 2006, **441**, 1179–1185.
2 H. M. Shapiro, *Practical flow cytometry*, Wiley-Liss, New York, 2003.
3 S. Koster, F. E. Angile, H. Duan, J. J. Agresti, A. Wintner, C. Schmitz, A. C. Rowat, C. A. Merten, D. Pisignano, A. D. Griffiths and D. A. Weitz, *Lab Chip*, 2008, **8**, 1110–1115.
4 J. F. Edd, D. Di Carlo, K. J. Humphry, S. Koster, D. Irimia, D. A. Weitz and M. Toner, *Lab Chip*, 2008, **8**, 1262–1264.
5 S. L. Anna, N. Bontoux and H. A. Stone, *Appl. Phys. Lett.*, 2003, **82**, 364–364.
6 L.-Y. Chu, A. S. Utada, R. K. Shah, J.-W. Kim and D. A. Weitz, *Angew. Chem., Int. Ed.*, 2007, **46**, 8970–8974.
7 R. K. Shah, H. C. Shum, A. C. Rowat, D. Lee, J. J. Agresti, A. S. Utada, L.-Y. Chu, J.-W. Kim, A. Fernandez-Nieves, C. J. Martinez and D. A. Weitz, *Mater. Today*, 2008, **11**, 18–27.
8 A. R. Abate and D. A. Weitz, *Small*, 2009, **24**, 24.
9 K. Ahn, C. Kerbage, T. P. Hunt, R. M. Westervelt, D. R. Link and D. A. Weitz, *Appl. Phys. Lett.*, 2006, **88**, 024104–024103.
10 J. C. Baret, O. J. Miller, V. Taly, M. Ryckelynck, A. El-Harrak, L. Frenz, C. Rick, M. L. Samuels, J. B. Hutchison, J. J. Agresti, D. R. Link, D. A. Weitz and A. D. Griffiths, *Lab Chip*, 2009, **9**, 1850–1858.
11 J. Clausell-Tormos, D. Lieber, J. C. Baret, A. El-Harrak, O. J. Miller, L. Frenz, J. Blouwolff, K. J. Humphry, S. Koster, H. Duan, C. Holtze, D. A. Weitz, A. D. Griffiths and C. A. Merten, *Chem. Biol.*, 2008, **15**, 427–437.
12 M. M. Wang, E. Tu, D. E. Raymond, J. M. Yang, H. Zhang, N. Hagen, B. Dees, E. M. Mercer, A. H. Forster, I. Kariv, P. J. Marchand and W. F. Butler, *Nat. Biotechnol.*, 2005, **23**, 83–87.
13 A. Y. Fu, C. Spence, A. Scherer, F. H. Arnold and S. R. Quake, *Nat. Biotechnol.*, 1999, **17**, 1109–1111.
14 P. S. Dittrich and P. Schwille, *Anal. Chem.*, 2003, **75**, 5767–5774.
15 C. Eckart, *Phys. Rev.*, 1948, **73**, 68.
16 W. L. Nyborg, in *Physical Acoustics, Properties of polymers and nonlinear acoustics*, ed. W. P. Mason, Academic Press, New York, 1965, vol. 2B.
17 Z. Guttenberg, H. Muller, H. Habermuller, A. Geisbauer, J. Pipper, J. Felbel, M. Kielpinski, J. Scriba and A. Wixforth, *Lab Chip*, 2005, **5**, 308–317.
18 T. Franke, A. R. Abate, D. A. Weitz and A. Wixforth, *Lab Chip*, 2009, **9**, 2625, DOI: 10.1039/b906819h.
19 T. Frommelt, M. Kostur, M. Wenzel-Schafer, P. Talkner, P. Hanggi and A. Wixforth, *Phys. Rev. Lett.*, 2008, **100**, 034502.
20 K. Sritharan, C. J. Strobl, M. F. Schneider, A. Wixforth and Z. Guttenberg, *Appl. Phys. Lett.*, 2006, **88**, 054102.
21 J. Shi, X. Mao, D. Ahmed, A. Colletti and T. J. Huang, *Lab Chip*, 2008, **8**, 221–223.
22 P. Augustsson, J. Persson, S. Ekstrom, M. Ohlin and T. Laurell, *Lab Chip*, 2009, **9**, 810–818.
23 J. Shi, H. Huang, Z. Stratton, Y. Huang and T. J. Huang, *Lab Chip*, 2009, **9**, 3354.
24 J. Shi, D. Ahmed, X. Mao, S. C. S. Lin, A. Lawit and T. J. Huang, *Lab Chip*, 2009, **9**, 2890–2895.
25 M. Wiklund and H. M. Hertz, *Lab Chip*, 2006, **6**, 1279–1292.
26 F. Petersson, L. Aberg, A.-M. Sward-Nilsson and T. Laurell, *Anal. Chem.*, 2007, **79**, 5117–5123.
27 S. Kapishnikov, V. Kantsler and V. Steinberg, *J. Stat. Mech.: Theory Exp.*, 2006, **2006**, P01012–P01012.
28 L. Johansson, F. Nikolajeff, S. Johansson and S. Thorslund, *Anal. Chem.*, 2009, **81**, 5188–5196.
29 J. C. Bischof, J. Padanilam, W. H. Holmes, R. M. Ezzell, R. C. Lee, R. G. Tompkins, M. L. Yarmush and M. Toner, 1995, 68, pp. 2608–2614.
30 M. M. Roden, K.-H. Lee, M. C. Panelli and F. M. Marincola, *J. Immunol. Methods*, 1999, **226**, 29–41.